RSC Advances

PAPER

View Article Online
View Journal | View Issue

Cite this: *RSC Adv.*, 2025, **15**, 29023

Catalytic isomerization of branched allylic alcohols by water-soluble $[RuCp(OH_2)(PTA)_2](CF_3SO_3)$ and $[RuCp(OH_2)(mPTA)_2](CF_3SO_3)_3$

Belén López-Sánchez, Franco Scalambra, Judit Cano-Asensio and Antonio Romerosa *

The isomerization of substituted allylic alcohols, including α-vinyl benzyl alcohol, *trans*-1,3-diphenyl-2-propen-1-ol, cinnamyl alcohol, coniferyl alcohol, 4-nitrocinnamyl alcohol, farnesol, 1,5-hexadien-3,4-diol, (1*R*)-(−)-myrtenol and *S*,*R*-(−)-carveol, catalyzed by the $[RuCp(OH_2)(PTA)_2](CF_3SO_3)$ (**1**) and $[RuCp(OH_2)(mPTA)_2](CF_3SO_3)_3$ (**2**) (PTA = 1,3,5-triaza-7-phosphaadamantane, mPTA = *N*-methyl-1,3,5-triaza-7-phosphaadamantane) complexes was examined in pure water and water-containing media. The isomerization of the chalcone *trans*-1,3-diphenyl-2-propen-1-ol catalyzed by **1** to produce the natural product propiophenone displays the highest known turnover number for this reaction to date (TON = 200 and $TOF_{5h} = 40\ h^{-1}$). A study delving into the catalytic reaction mechanisms was carried out, aiming to understand the influence of different functional groups on the studied isomerization processes. The intermediates of the isomerization of α-vinylbenzyl alcohol and 1,5-hexadien-3,4-diol catalyzed by **1** and **2** were isolated and characterized by NMR spectroscopy.

Received 20th May 2025
Accepted 3rd August 2025

DOI: 10.1039/d5ra03564c

rsc.li/rsc-advances

Introduction

In the last decades, it was proven that allylic alcohols can be conveniently converted into their respective carbonyl compounds *via* one-step isomerization reactions catalyzed by suitable metal complexes under mild conditions and in harmless solvents such as water.[1,2] This synthetic process is influenced by the size of the substrate and the substituents on the double bond.[3] However, although numerous transition metal complexes[4–7] have been found to be useful in isomerizing linear allylic alcohols,[8–10] the number that can be employed for the isomerization of substituted allylic alcohols is considerably lower. Particularly, the list of catalysts for the isomerization of allylic alcohols bearing bulky groups is notably short, and in some instances, no example has been described. In this regard, the evaluation of water-soluble catalysts for the isomerization of branched allylic alcohols could be a sustainable and environmentally friendly approach, achieving significant products with potential applications in medicinal and fine chemistry, as well as in the field of natural products.[11]

Ruthenium complexes featuring hydrophilic tertiary organophosphine ligands,[12] such as triphenylphosphines (Na-mTPPMS and Na_3-mTPPTS),[13] and the adamantane-like ligand 1,3,5-triaza-7-phosphaadamantane (PTA) and derivatives[14–16] are among the wide variety of catalysts used. To date, the efficacy of various water-soluble ruthenium complexes containing PTA and its monomethylated derivative mPTA (*N*-methyl-1,3,5-triaza-7-phosphaadamantane) has been supported by several significant results.[17–21] In particular, the $[RuCp(OH_2)(PTA)_2](CF_3SO_3)$ (**1**) and $[RuCp(H_2O)(mPTA)_2](CF_3SO_3)_3$ (**2**) complexes are active catalysts for isomerizing a wide variety of linear[20–24] and cyclic[25–27] allylic alcohols in aqueous environments (Scheme 1). Despite the similarities in the structure and composition of these complexes, they display significant catalytic differences such as conversion and a better reaction medium.[20,21,27]

It is important to note that complex **1** was found to be useful for the easy synthesis of some pheromones[28–38] involved in the natural aggregation/anti-aggregation system of the Douglas-fir beetle (*Dendroctonus pseudotsugae*), which is known to be the

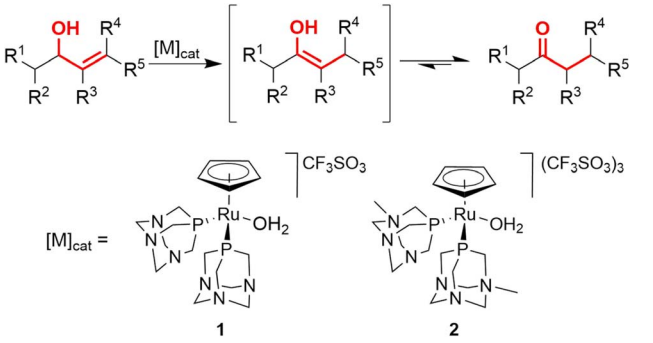

Scheme 1 Isomerization of allylic alcohols catalysed by ruthenium complexes bearing PTA (**1**) and mPTA (**2**).

Área de Química Inorgánica-CIESOL, Universidad de Almería, Almería, Spain. E-mail: romerosa@ual.es

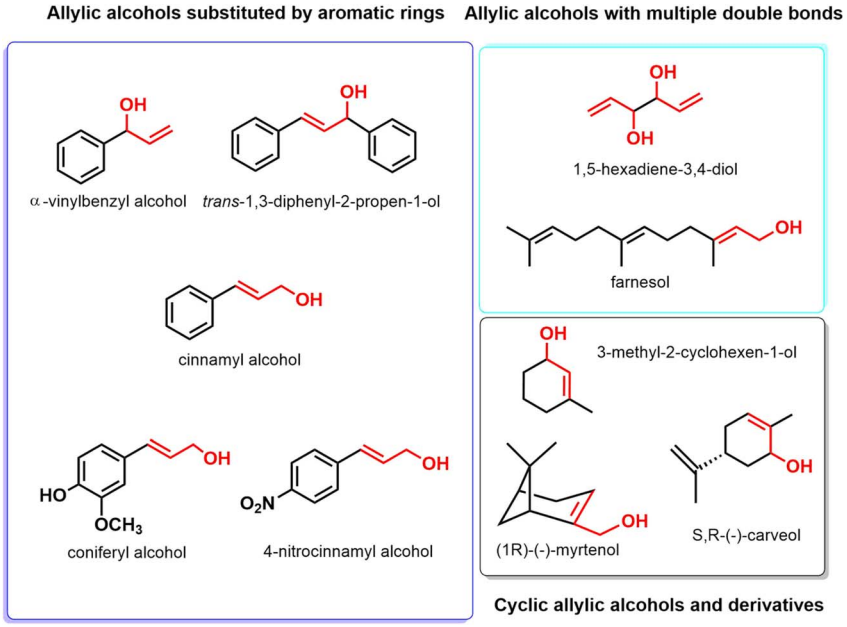

Fig. 1 Substituted allylic alcohols evaluated for catalytic isomerization in aqueous media.

major killer of conifers.[39] Therefore, the study of the catalytic properties of these complexes not only provides a new insight about how the substituents of the allylic alcohols influence their catalytic activity in aqueous media, but also provides new useful synthetic procedures for obtaining valuable compounds.

Herein, the catalytic applications of **1** and **2** were studied in water and reaction media containing water (henceforth denoted as aqueous media) for the isomerization of allylic alcohols bearing unsubstituted and substituted aromatic rings and/or multiple double bonds, including α-vinylbenzyl alcohol, cinnamyl alcohol, *trans*-1,3-diphenyl-2-propen-1-ol, coniferyl alcohol, and 4-nitrocinnamyl alcohol, farnesol and 1,5-hexadien-3,4-diol. Finally, the cyclic allylic alcohols 3-methyl-2-cyclohexen-1-ol, (1*R*)-(−)-myrtenol and *S*,*R*-(−)-carveol were also tested (Fig. 1). Most of them and/or their isomerization products come from can be in found natural resources,[40–42] such as essential oils.[43–45] They play pivotal roles as starting materials or major components in food,[40,46] fragrances,[47,48] pharmaceuticals[49–51] or synthetic applications.[52,53] For instance, (1*R*)-(−)-myrtenol, found in certain aromatic plants, is used in the fragrance[54,55] and pharmaceutical industries due to its anti-inflammatory, antioxidant and antimicrobial properties.[56–58] Similarly, cinnamyl alcohol, found in plants such as cinnamon,[59,60] is widely used in the fragrance, cosmetics and deodorant industries,[48] as well as an intermediate compound in various manufacturing processes.[61]

This study represents the first example of the use of water-soluble cyclopentadienyl Ru(II) complexes bearing phosphine ligands for the isomerisation of these allylic alcohols. Related systems found in the literature include Ru(II)-arene complexes such as $[RuCl_2(mTHPA)(\eta^6\text{-}C_6H_6)]$ (mTHPA = *N*-methyl-trihydrazinophosphaadamantane),[12] as well as complexes featuring substituted hydroxyethoxy-arene and phosphine ligands, for example $[RuCl_2(\eta^6\text{-}C_6H_5OCH_2CH_2OH)P(OMe)_3]$ and $[RuCl_2(\eta^6\text{-}C_6H_5OCH_2CH_2OH)P(O^iPr)_3]$.[62] Additionally, a heterodimetallic Ru/Fe complex, $[Ru(\eta^6\text{-}p\text{-cymene})Cl_2$(1-(diphenylphosphanyl)-1'-[*N*-(2-hydroxyethyl)-carbamoyl]ferrocene-κP)], has been reported.[63] Several Ru(IV) complexes bearing the 2,7-dimethylocta-2,6-diene and dodeca-2,6,10-triene ligands have been studied, including $[Ru(\eta^3\text{:}\eta^3\text{-}C_{10}H_{16})Cl(\kappa^2O,O\text{–}CH_3CO_2)]$,[3] $[Ru(\eta^3\text{:}\eta^3\text{-}C_{10}H_{16})(Cl)_2$(pyrazole)],[64] $[Ru(\eta^3\text{:}\eta^3\text{-}C_{10}H_{16})(Cl)_2$(benzimidazole)],[65,66] and $[Ru(\eta^3\text{:}\eta^2\text{:}\eta^3\text{-}C_{12}H_{18})Cl_2]$.[62] In the case of Rh-complexes, catalytic systems formed by the combination of $[Rh(COD)Cl]_2$ with the phosphine PTA or aryl sulfonated phosphines have also been reported.[7]

Results and discussion

Catalytic reactions

Linear allylic alcohols containing aromatic rings: *trans*-1,3-diphenyl-2-propen-1-ol, α-vinylbenzyl alcohol, cinnamyl alcohol, 4-nitrocinnamyl alcohol, and coniferyl alcohol.

The isomerization of *trans*-1,3-diphenyl-2-propen-1-ol into dihydrochalcone was performed in CH_3OH/H_2O (1 : 1) at 70 °C and $^iPrOH/H_2O$ (1 : 1) at 80 °C, with varying catalyst loadings (Table S1). Table 1 summarizes the results obtained, along with a comparison with published catalysts. It is significant to stress that complete substrate conversion was achieved within 4 h using 1 mol% of **1** in CH_3OH/H_2O (TOF_{4h} = 24.8 h^{-1}). Decreasing the catalyst to 0.2 mol% in $^iPrOH/H_2O$ resulted in 40% conversion (TOF_{5h} = 40 h^{-1}) after 5 h. In contrast, 1 mol% of **2** in $MeOH/H_2O$ failed to isomerize the substrate, as no more than 5% conversion (TOF_{4h} = 2.6 h^{-1}) was obtained in 4 h. Therefore, the catalyst loading was increased to 10 mol%, leading to a conversion of 53% in 24 h (TOF_{24h} = 0.22 h^{-1}). Dihydrochalcone was obtained with 99% conversion. The resulting pure product was characterized by ^1H NMR (Fig. S81). It was obtained by extracting the reaction mixture with $CHCl_3$,

Table 1 Catalytic isomerization of *trans*-1,3-diphenyl-2-propen-1-ol into dihydrochalcone by **1** and **2**: comparison with bibliographic results

trans-1,3-diphenyl-2-propen-1-ol dihydrochalcone

Catalyst	[Cat] mol%	*T* (h)	*T* (°C)	Solvent	Additive	TOF[a] (h^{-1})	Conversion (%)	Ref.
1	1	2	70	$MeOH/H_2O$	—	37.5	75	This work
1	1	4	70	$MeOH/H_2O$	—	24.8	>99	This work
1	0.2	5	70	$MeOH/H_2O$	—	12.4	12.4	This work
1	0.2	5	80	$^{i}PrOH/H_2O$	—	40	40	This work
2	1	2	70	$MeOH/H_2O$	—	2.6	5	This work
[Ru(η^6-*p*-cymene)Cl_2(1-(diphenylphosphanyl)-1′-[*N*-(2-hydroxyethyl)-carbamoyl]ferrocene-κP)]	2	20	80	H_2O	KOtBu	2.5	99	63

[a] TOF = turn over frequency, N_2, ROH/H_2O (1 : 1) = 1 mL, % measured by ^1H NMR.

drying over $CaCl_2$, filtering the collected organic layers through a silica gel column, and drying under vacuum overnight.

Although the catalytic redox isomerization of *trans*-1,3-diphenyl-2-propen-1-ol has been extensively reviewed in organic media, fewer studies were reported in aqueous environments, where a heterodimetallic Ru/Fe complex is the most efficient catalyst in water reported so far, achieving TON = 49 and TOF = 2.5 h^{-1} at 80 °C and in the presence of KO^{t}Bu.[63] Thus, complex **1** showed the best catalytic profile for this reaction in terms of both TON and TOF.

The isomerization of α-vinylbenzyl alcohol into propiophenone was evaluated under the same conditions as the previous substrate in CH_3OH/H_2O (1 : 1) at 70 °C or $^{i}PrOH/H_2O$ (1 : 1) at 80 °C (Table S2). Using 1 mol% of **1** or **2** in CH_3OH/H_2O (1 : 1), 40% conversion into propiophenone was achieved in both cases after 24 h ($TOF_{24h} = 1.7\ h^{-1}$). Changing the solvent to $^{i}PrOH/H_2O$ (1 : 1) resulted in higher and faster transformation into propiophenone, achieving a conversion of 44% with **1** at 8 h ($TOF_{8h} = 5.5\ h^{-1}$) and of 71% with **2** ($TOF_{8h} = 8.9\ h^{-1}$). Increasing the catalyst loading of both complexes to 2 mol% led to complete isomerization, in both CH_3OH/H_2O (1 : 1) and $^{i}PrOH/H_2O$ (1 : 1), and evidenced that complex **2** is more active (CH_3OH/H_2O (1 : 1): $TOF_{4h} = 3.1\ h^{-1}$; $^{i}PrOH/H_2O$ (1 : 1): $TOF_{1h} = 34.5\ h^{-1}$, $TOF_{4h} = 12.4\ h^{-1}$) than **1** (CH_3OH/H_2O (1 : 1): $TOF_{4h} = 3.3\ h^{-1}$; $^{i}PrOH/H_2O$ (1 : 1): $TOF_{4h} = 8.4\ h^{-1}$, $TOF_{8h} = 6.2\ h^{-1}$). Complex **2** clearly showed higher activity in the $^{i}PrOH/H_2O$ (1 : 1) mixture than in CH_3OH/H_2O (1 : 1). Propiophenone synthesis was achieved with 99% conversion. The process was the same as that used to obtain dihydrochalcone. Its characterization by ^1H NMR is shown in Fig. S82.

As shown in Table 2, previously published results showed that some Ru(II) and various Ru(IV) complexes and Rh complexes exhibit notable catalytic activity for the isomerization of α-vinylbenzyl alcohol in aqueous media.[3,7,62,64–67] The most notable contribution was the Ru(IV) complex bearing η^3:η^3-$C_{10}H_{16}$ and a bidentate acetate ligand, [Ru(η^3:η^3-$C_{10}H_{16}$)Cl(κ^{2}O,O–CH_3CO_2)], which was found to be a highly efficient catalyst for this reaction in water at 75 °C (TON = 99, TOF = 1200 h^{-1}).[3] Other studies include the complex [Ru(η^3:η^3-$C_{10}H_{16}$)(Cl)$_2$(-pyrazole)], which also achieved high TOF values (495 h^{-1}) in water at 75 °C (TON = 99);[64] and/or the [Ru(η^3:η^3-$C_{10}H_{16}$)(-Cl)$_2$(benzimidazole)] complex[65] in KH_2PO_4 phosphate buffer containing $MgSO_4$ (39.6 h^{-1}, TON = 99) at 50 °C.[66] The Ru(IV)-complex [Ru(η^3:η^2:η^3-$C_{12}H_{18}$)Cl_2] also exhibited high catalytic activity for the transformation of this allylic alcohol, with TOF values of 20 h^{-1} (TON = 99) in water and 80 (TON = 99) in H_2O/$CsCO_3$ at 75 °C.[62] Among the Ru(II) compounds, the Ru-arene complex bearing mTHPA, [$RuCl_2$(mTPHA)(η^6-C_6H_6)], proved to be a suitable catalyst for this reaction in water with KO^{t}Bu at 75 °C (TON = 97, TOF = 129 h^{-1}).[12] However, the highest catalytic activity for this reaction with Ru(II)-arene complexes was obtained with [$RuCl_2$(η^6-$C_6H_5OCH_2CH_2OH$)P(OMe)$_3$] and [$RuCl_2$(η^6-$C_6H_5OCH_2CH_2OH$)P(O^{i}Pr)$_3$], achieving both of them TOF values of 600 h^{-1} (TON = 99) in water and KO^{t}Bu at 75 °C.[62] Regarding the Rh-complexes, active catalytic systems were generated *in situ* upon using [Rh(COD)Cl]$_2$ and PTA or aryl sulfonated phosphines as cocatalysts, affording the highest activity when PTA was used.[7] It is important to stress that complexes **1** and **2** are also the first Ru(II)-cyclopentadienyl complexes evaluated for this reaction in water, and although the results show that they are efficient and useful for this reaction, they do not equal or surpass previously published catalysts.

The catalytic isomerization of cinnamyl alcohol to obtain hydrocinnamaldehyde showed that both catalysts display a performance significantly lower than that previously published in the literature in aqueous media (Table 3).[3,7,62,64,65,67] No conversion was observed in CH_3OH/H_2O (1 : 1) at 70 °C, with 1 mol% of both complexes, and also in $^{i}PrOH/H_2O$ (1 : 1) at 80 °C with 10% of catalyst, the conversion remained very low after 24 h (**1** : 5% and **2** : 11%) (Table S3). However, some of the Ru(IV) and Rh complexes reported in the literature are more efficient for the isomerization of cinnamyl alcohol in aqueous media, where the most active Ru(IV)-complex is [Ru(η^3:η^3-$C_{10}H_{16}$)(-Cl)$_2$(benzimidazole)] in phosphate buffer containing $^{i}PrNH_2$ at

Table 2 Catalytic isomerization of α-vinylbenzyl alcohol into propiophenone by **1** and **2**, including significant bibliographic results

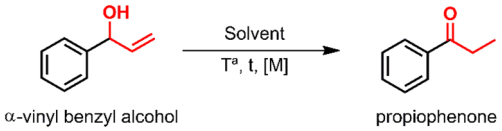

Catalyst	[Cat] mol%	t (h)	T (°C)	Solvent	Additive	TOF[a] (h^{-1})	Conversion (%)	Ref.
1	1	8	70	$MeOH/H_2O$	—	3.5	28	This work
1	1	8	80	$^iPrOH/H_2O$	—	5.5	44	This work
1	2	4	70	$MeOH/H_2O$	—	3.1	25	This work
1	2	8	70	$MeOH/H_2O$	—	2.6	41	This work
1	2	4	80	$^iPrOH/H_2O$	—	8.4	67	This work
1	2	8	80	$^iPrOH/H_2O$	—	6.2	99	This work
2	1	24	70	$MeOH/H_2O$	—	1.7	40	This work
2	1	24	80	$^iPrOH/H_2O$	—	3.1	73	This work
2	2	4	80	$MeOH/H_2O$	—	3.5	28	This work
2	2	8	80	$MeOH/H_2O$	—	2.6	42	This work
2	2	1	80	$^iPrOH/H_2O$	—	34.5	69	This work
2	2	4	80	$^iPrOH/H_2O$	—	12.4	>99	This work
$[Rh(COD)Cl]_2$	5	17	80	H_2O	MeO-TPPMS	1.2	99	7
$[Rh(COD)Cl]_2$	5	18	80	H_2O	PTA NaOH	1.1	99	7
$[Rh(COD)(CH_3CN)_2]BF_4$	2	0.08	23	H_2O	PTA NaOH	594	99	7
$[RuCl_2(mTHPA)(\eta^6\text{-}C_6H_6)]$	1	0.75	75	H_2O	KO^tBu	129	97	12
$[RuCl_2(\eta^6\text{-}C_6H_5OCH_2CH_2OH)(P(O^iPr)_3)]$	1	10	75	H_2O	KO^tBu	600	99	62
$[\{Ru(\eta^3\text{:}\eta^3\text{-}C_{10}H_{16})(\mu\text{-}Cl)Cl_2\}]$	5	1	75	H_2O	—	20	99	62
$[\{Ru(\eta^3\text{:}\eta^3\text{-}C_{10}H_{16})(\mu\text{-}Cl)Cl_2\}]$	5	0.25	75	H_2O/Cs_2CO_3	—	80	99	62
$[Ru(\eta^3\text{:}\eta^3\text{-}C_{10}H_{16})(Cl)_2(benzimidazole)]$	1	3 h	50	H_2O	$^iPrNH_2$ KH_2PO_4 buffer	33	99	67
$[Ru(\eta^3\text{:}\eta^3\text{-}C_{10}H_{16})(Cl)_2(benzimidazole)]$	1	0.25	75	H_2O	—	396	99	65
$[Ru(\eta^3\text{:}\eta^3\text{-}C_{10}H_{16})(Cl)_2(pyrazole)]$	0.2	1	75	H_2O	—	495	99	64
$[Ru(\eta^3\text{:}\eta^3\text{-}C_{10}H_{16})Cl(\kappa^2O,O\text{–}CH_3CO_2)]$	1	2.5	50	H_2O	$MgSO_4$ KH_2PO_4 buffer	39.6	99	66
$[Ru(\eta^3\text{:}\eta^3\text{-}C_{10}H_{16})Cl(benzimidazole)]$	1	2.5	50	H_2O	$MgSO_4$ KH_2PO_4 buffer	39.6	99	66
$[Ru(\eta^3\text{:}\eta^3\text{-}C_{10}H_{16})Cl(\kappa^2O,O\text{–}CH_3CO_2)]$	1	0.08	75	H_2O	—	1200	99	3

[a] TOF = turn over frequency, N_2, ROH/H_2O (1 : 1) = 1 mL, % measured by ^1H NMR.

50 °C (TON = 99, TOF = 33 h^{-1})[67] and the most active reported Rh-complex is $[Rh(COD)(CH_3CN)_2]BF_4$ in the presence of PTA in H_2O at 45 °C (TON = 29.5, TOF = 39.3 h^{-1}).[7]

In view of the obtained results for the catalytic isomerization of allylic alcohols containing unsubstituted aromatic compounds, the catalytic isomerization of some examples of *para*-phenyl-substituted allylic alcohols was assessed. Thus,

Table 3 Catalytic isomerization of cinnamyl alcohol into hydrocinnamaldehyde alcohols by **1** and **2**: comparison with bibliographic results

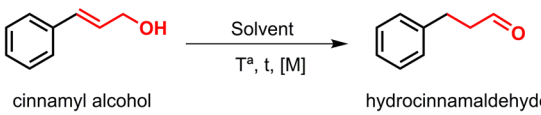

Catalyst	[Cat] mol%	t (h)	T (°C)	Solvent	Additive	TOF[a] (h^{-1})	Conversion (%)	Ref.
1	10	24	80	$^iPrOH/H_2O$	—	0.02	5	This work
2	10	24	80	$^iPrOH/H_2O$	—	0.05	11	This work
$[Rh(COD)(CH_3CN)_2]BF_4$	2	0.75	45	H_2O	PTA	39.3	59	7
$[\{Ru(\eta^3\text{:}\eta^3\text{-}C_{10}H_{16})(\mu\text{-}Cl)Cl_2\}]$	10	3	75	H_2O	—	3	99	68
$[\{Ru(\eta^3\text{:}\eta^3\text{-}C_{10}H_{16})(\mu\text{-}Cl)Cl_2\}]$	10	2.5	75	H_2O/Cs_2CO_3	—	4	99	68
$[Ru(\eta^3\text{:}\eta^3\text{-}C_{10}H_{16})Cl(\kappa^2O,O\text{–}CH_3CO_2)]$	5	2	75	H_2O	—	7	74	3
$[Ru(\eta^3\text{:}\eta^3\text{-}C_{10}H_{16})(Cl)_2(benzimidazole)]$	5	2.5	75	H_2O	—	4	50	65
$[Ru(\eta^3\text{:}\eta^3\text{-}C_{10}H_{16})(Cl)_2(benzimidazole)]$	1	4	50	H_2O	$^iPrNH_2$ KH_2PO_4 buffer	33	99	67
$[Ru(\eta^3\text{:}\eta^3\text{-}C_{10}H_{16})(Cl)_2(pyrazole)]$	5	1	75	H_2O	—	9.4	47	64

[a] TOF = turn over frequency, N_2, ROH/H_2O (1 : 1) = 1 mL, % measured by ^1H NMR.

catalytic isomerization of 4-nitrocinnamyl alcohol and coniferyl alcohol into 3,4-nitrobenzenepropanal and dihydroconiferyl aldehyde, respectively, was evaluated with complexes **1** and **2**. No conversion of the substrates into dihydroconiferyl aldehyde was observed under the tested conditions in CH_3OH/H_2O (1 : 1) at 70 °C and $^{i}PrOH/H_2O$ (1 : 1) at 80 °C. Nevertheless, minor conversion (<5%) for the isomerization of 4-nitrocinnamyl alcohol was achieved with 10 mol% of both catalysts after 48 h (Table S4), which is a very low conversion, but it is the first reported for this substrate to the best of our knowledge.

Linear allylic alcohols containing multiple double bonds: farnesol and 1,5-hexadiene-3,4-diol. The catalytic efficiency of both complexes was evaluated against farnesol and 1,5-hexadiene-3,4-diol. Despite employing a high catalyst loading of 10 mol%, the isomerization of farnesol in CH_3OH/water (1 : 1) at 75 °C did not occur, and in $^{i}PrOH/H_2O$ (1 : 1) at 80 °C, only a low conversion to dihydrofarnesal was obtained after 48 h (**1** : 3%; **2** : 1%). Likewise, the isomerization of 1,5-hexadiene-3,4-diol in methanol at 70 °C and in water up to 100 °C did not occur (Table S5).

Cyclic allylic alcohols: 3-methyl-2-cyclohexen-1-ol, *S*,*R*-(−) carveol and (1*R*)-(−)-myrtenol. The last group of substrates tested included the cyclic allylic alcohols 3-methyl-2-cyclohexen-1-ol, *S*,*R*-(−)-carveol, and (1*R*)-(−)-myrtenol. We showed that complex **1** exhibited very high activity for the catalytic isomerization of 2-cyclohexen-1-ol into cyclohexenone (H_2O: TOF = 324 h^{-1}; CH_3OH: TOF = 49 h^{-1}; H_2O/cyclohexane: TOF = 163 h^{-1})[25] and 3-methyl-2-cyclohexen-1-ol into 3-methylcyclohexenone (H_2O: TOF_{5h} = 17 h^{-1}; CH_3OH: TOF_{2h} = 17 h^{-1}).[26] The activity of **2** in the isomerization of 2-cyclohexen-1-ol was also evaluated, obtaining good results,[27] although inferior to that obtained with complex **1**.[25] Table S6 summarizes the reaction conditions for the isomerization of 3-methyl-2-cyclohexen-1-ol in the presence of **1** and **2**, where it is also observed that for this reaction, complex **2** is less active than **1**. With 1 mol% of **2** in methanol no isomerization was observed, and in water only 18% conversion was achieved after 5 h (TOF_{5h} = 3.6 h^{-1}). Similarly, the isomerization of *S*,*R*-(−)-carveol did not proceed employing 10 mol% of both complexes (Table S7). Notably, the catalytic isomerization of (1*R*)-(−)-myrtenol with 10 mol% of **1** in $^{i}PrOH/H_2O$ (1 : 1) at 80 °C achieved a conversion of 70% after 48 h (TOF_{48h} = 0.15 h^{-1}), while with **2** the conversion was 43% (TOF_{48h} = 0.1 h^{-1}) (Table 4). Myrtanal was obtained from (1*R*)-(−)-myrtenol with a conversion of 70%. The process was the same as that followed to obtain dihydrochalcone and propiophenone. The resulting mixture was characterized by ^{1}H NMR, as shown in Fig. S84. It is important to stress that to the best of our knowledge, this is the first example of the isomerization of this alcohol in aqueous media at 80 °C.[69]

Catalytic isomerization mechanism

Study of the reactivity of branched allylic alcohols against 1 and 2. To gain a better understanding of the isomerization of the studied allylic alcohols, representative catalytic reactions were studied by $^{31}P\{^1H\}$ NMR and ^{1}H NMR in D_2O and CD_3OD/D_2O (2 : 1) in a 5 mm NMR tube. In the latter solvent mixture, complexes **1** and **2** are in substitutional equilibrium with methanol, forming a certain amount of the respective $[RuCpL_2(CD_3OD)]^{n+}$ (L: PTA, n = 2, $\delta^{31}P$ = −25.8 ppm; mPTA, n = 2, $\delta^{31}P$ = −10.3 ppm). Additionally, complex **2** partially deprotonates into $[RuCp(OD)(mPTA)_2]^{2+}$, which is characterized by a singlet at −8.6 ppm.[20,27]

Regarding the study of the reactions with the substrates (1*R*)-(−)-myrtenol, *S*,*R*-(−)-carveol, farnesol, 4-nitrocinnamyl alcohol, farnesol, and coniferyl alcohol, in which a range of modest to no conversion was observed, no additional signals were detected in the $^{31}P\{^1H\}$ and ^{1}H NMR spectra even after 72 h at 80 °C, apart from the abovementioned signals, which is a consequence of the reaction with the solvent media. The lack of isomerization of (1*R*)-(−)-myrtenol and *S*,*R*-(−)-carveol, but also of observable intermediates, is likely due to steric hindrance. These substrates are constituted by bulky substituents, such as a bicyclic group in the case of (1*R*)-(−)-myrtenol and a methyl group at the vinyl position in *S*,*R*-(−)-carveol, which is also a cyclic substrate. These bulky substituents make difficult the coordination of the allylic alcohols to the metal centre by the

Table 4 Catalytic isomerization of (1*R*)-(−)-myrtenol into myrtanal catalyzed by **1** and **2**

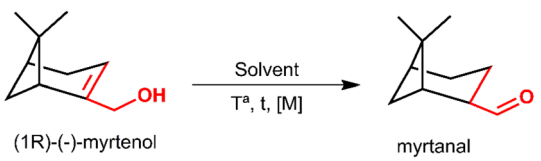

Catalyst	[Ru] mol%	T (°C)	Time (h)	Solvent	TON	TOF[a] (h^{-1})	Conversion (%)
1	10	70	8	$MeOH/H_2O$	3	0.4	30
1	10	80	8	$^{i}PrOH/H_2O$	3.5	0.4	35
1	10	80	48	$^{i}PrOH/H_2O$	7.0	0.2	70
2	10	80	24	$^{i}PrOH/H_2O$	2.5	0.1	25
2	10	80	48	$^{i}PrOH/H_2O$	4.3	0.1	43

[a] TON = turn over number, TOF = turn over frequency, N_2, ROH/H_2O 1 : 1 = 1 mL, % measured by ^{1}H NMR.

double bond and OH. The substrates 4-nitrocinnamyl alcohol and coniferyl alcohol also have bulky groups in their structure. Alternatively, farnesol has a long chain containing methyl groups and multiple double bonds, which compete with the allylic C=C group for coordination with the metal. Finally, it seems that when the phenyl groups are in the vinyl position and para-substituted with electron-withdrawing groups, the isomerization process is hindered. Nevertheless, despite being substituted alkenes, 3-methyl-2-cylohexen-1-ol, *trans*-1,3-diphenyl-2-propen-1-ol, cinnamyl alcohol, α-vinyl benzyl alcohol and 1,5-hexadien-3,4-diol underwent transformations. The follow-up reactions of 3-methyl-2-cylohexen-1-ol with **2** both in CD_3OD and in D_2O are illustrated in Fig. S1–S4. Notably, the $^{31}P\{^1H\}$ NMR spectra over time suggested the decomposition of **2** as the signal at −10.3 ppm decreased, but no additional peak appeared. In contrast, the catalyst gave rise to new species different from that expected by reaction with the solvent when the catalytic isomerization of *trans*-1,3-diphenyl-2-propen-1-ol with **1** (Fig. S5–S8) was studied by $^{31}P\{^1H\}$ NMR (Fig. S6), which are assigned to O=PTA (−7.2 ppm) and $[RuCpH(PTA)_2]$ (−10.73 ppm).[70,71] Nevertheless, no signals ascribed to reaction intermediates were observed. Considering that this catalyst facilitates the isomerization more effectively and faster than **2**, the obtained results suggest that once the respective intermediates are formed, they evolve faster than possible to be determined by NMR. Although this is also a bulky substrate, its electron-withdrawing group in the allylic position appears to aid the isomerisation process. Besides the abovementioned substrates, the study of the catalytic isomerization with **1** of cinnamyl alcohol (Fig. S9 and S10) showed that two doublets arise in the $^{31}P\{^1H\}$ NMR spectra. Their weak abundance prevented the complete characterization of these species, but their chemical shifts at −26.9 ppm and −36.6 ppm, together with the magnitude of their coupling constant of $^2J_{PP}$ = 46.0 Hz, suggested that the CH=CH group of cinnamyl alcohol is coordinated to the metal, similar to that found with 1,5-hexenadien-3,4-diol and α-vinyl benzyl alcohol.

α-Vinylbenzyl alcohol was tested in CD_3OD/D_2O (2 : 1) at 70 °C and at room temperature with both complexes **1** and **2** (Fig. S11–S18). After 24 h, the ^1H NMR spectra evidence the formation of propiophenone (Fig. S11 and S13), while in the $^{31}P\{^1H\}$ NMR spectra, two sets of doublets appeared, corresponding to two AB systems located in the range of −21.6 ppm to −26.6 ppm in the reaction with **1**, and −6.0 ppm to 9.3 ppm with **2** (Fig. S12 and S14), respectively. Additionally, the $^{31}P\{^1H\}$ NMR spectra display two less intense singlets at −10.23 ppm and −12.39 ppm (<4%), which were not possible to characterize (Fig. S14). The proportion of the two sets of doublets was 8.3 : 1.7 in the reaction with **1**, and 7.5 : 2.5 in the reaction with **2**. At room temperature, no conversion of the substrate was observed (Fig. S15 and S17), but $^{31}P\{^1H\}$ NMR displayed the same peaks as that at 80 °C (Fig. S16 and S18). The reaction between α-vinylbenzyl alcohol and **2** in ^{i}PrOH/H_2O was monitored at 25 °C and 60 °C by $^{31}P\{^1H\}$ NMR experiments using a D_2O capillary (Fig. S19). At 25 °C, the $^{31}P\{^1H\}$ NMR spectrum exhibited four doublets (54%), in a 7.7 : 2.3 proportion, along with a singlet corresponding to complex **2** (46%), where the *exo*/*endo* ratio remained constant after heating to 60 °C.

The observed intermediates were synthesized and characterized as complexes $[RuCp(\eta^2\text{-}CH_2{=}CH{-}CHOH{-}C_6H_5)(PTA)_2](CF_3SO_3)$ (**3**) and $[RuCp(\eta^2\text{-}CH_2{=}CH{-}CHOH{-}C_6H_5)(mPTA)_2](CF_3SO_3)_3$ (**4**), which were obtained by reacting **1** and **2** with 50 eq. excess of α-vinylbenzyl alcohol in CH_3OH at room temperature and under N_2, followed by precipitation with diethyl ether (see SI, Section 9), respectively. Both complexes are stable in solution at room temperature up to 48 h under N_2 and were fully characterized by multinuclear NMR in CD_3OD (**3**: Fig. S32–S39 and **4**: Fig. S40–S46). The $^{31}P\{^1H\}$ NMR spectrum of **3** (Fig. S33) displays a set of four doublets between −23.00 ppm and −28.1 ppm, in an 8.7 : 1.3 ratio. In contrast, the $^{31}P\{^1H\}$ NMR spectrum of **4** (Fig. S41) only shows two doublets in the range of −6.0 to ppm −10.0 ppm, along with four other singlets (<25%), which were assigned to **2**, O = mPTA, $[RuCp(OH)(mPTA)_2]^{2+}$ and $[RuCp(OCD_3)(mPTA)_2]^+$. An

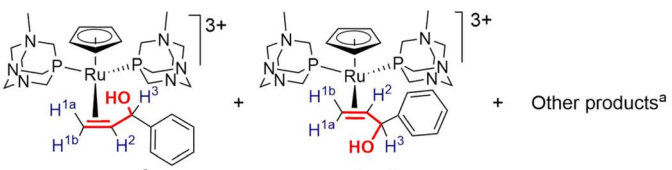

Solvent =	25	3.9	--	6.1
CD_3OD	60	1.9	--	8.1
Solvent =	25	4.6(8.7) [b]	0.9(1.3) [b]	4.5
CD_3OD/D_2O	60	1.2(8.6) [b]	0.1(1.4) [b]	8.7
Solvent =	25	5.1(8.5) [b]	0.9(1.5) [b]	4
^{i}PrOH/H_2O	60	1	--	9

Scheme 2 Reactivity of intermediate **4** in CD_3OD, CD_3OD/D_2O, and ^{i}PrOH/H_2O (D_2O capillary) at 25 °C and 60 °C. (a) In CD_3OD, other products correspond to **2**, $[RuCp(OCD_3)(mPTA)_2]^+$, O = mPTA, $[RuCp(OD)(mPTA)_2]^+$ and another unidentified species; in CD_3OD/D_2O or ^{i}PrOH/H_2O, other products correspond to 2, $[RuCp(OCD_3)(mPTA)_2]^+$ or $[RuCp(^i PrOH)(mPTA)_2]^+$. (b) Values in parentheses represent the exo/endo isomers ratio.

additional singlet at −12.1 ppm was also observed, which could not be characterized.

The study of both complexes by ^{1}H–^{1}H ROESY experiments suggests that **3** in solution is mainly the isomer *exo*-[RuCp(η^2-CH_2=CH–CHOH–C_6H_5)(PTA)$_2$][CF_3SO_3] (*exo*-**3**), as indicated by the correlation between the H^{1a} and H^3 protons to the Cp protons, while the minor species is *endo*-[RuCp(η^2-CH_2=CH–CHOH–C_6H_5)(PTA)$_2$][CF_3SO_3] (*endo*-**3**), where H^{1b} and H^2 are related to the Cp protons (Fig. S39). In contrast, only the *exo*-[RuCp(η^2-CH_2=CH–CHOH–C_6H_5)(mPTA)$_2$][CF_3SO_3]$_3$ (*exo*-**4**) was observed in CD_3OD, which was supported by the cross peaks related to H^{1a} and H^3 with Cp-H (Fig. S46 and 2). The *endo*-isomer was not detected, even at 60 °C, where only the transformation of complex **4** into **2**, [RuCp(OCD_3)(mPTA)$_2$]$^+$, O = mPTA, [RuCp(OH)(mPTA)$_2$]$^+$ and an unidentified species (−12.5 ppm) was observed (Fig. S47). Notably, the addition of D_2O to a methanolic solution of *exo*-**4** gave rise to the formation to two doublets corresponding to the *endo*-isomer (−7.19 ppm, d, mPTA, *endo*-**4**, $^2J_{PP}$ = 41.52 Hz) and −8.85 ppm; d, mPTA, *endo*-**4**, $^2J_{PP}$ = 41.52 Hz)), together with **2** and propiophenone (Fig. S48 and S49), respectively. The *endo*-isomer was characterized by multinuclear NMR in CD_3OD/D_2O 2 : 1 (Fig. S50–S58). The special disposition of this isomer was supported by the correlation between Cp-H and H^{1b} H^{-3} in the ^{1}H–^{1}H ROESY experiment (Fig. S58). The *exo*-**4**/*endo*-**4** proportion in 2 : 1 CD_3OD/D_2O was 8.7 : 1.3, evidencing the strong importance of water in triggering the *exo*/*endo* isomerization of **4**. In the temperature range of 25–60 °C the *exo*-**4**/*endo*-**4** ratio decreased to 8.6 : 1.4, releasing **2** and propiophenone (Scheme 2 and Fig. S59).

Furthermore, to understand why the substrate transformation catalyzed by **2** is more efficient in the mixture ^{i}PrOH/H_2O than in CH_3OH/H_2O, the same experiment was conducted by replacing CD_3OD with ^{i}PrOH (Fig. S60). In this solvent mixture, the *exo*/*endo* interconversion at room temperature shifted to the formation of *endo*-**4** (*exo*/*endo* ratio = 8.5 : 1.5). After heating for 15 min at 60 °C, only the transformation of *endo*-**4** into **2** and propiophenone was observed in the ^{31}P{^{1}H} NMR spectrum (Fig. S60). Although all tests conducted in the presence of water show the presence of the *exo* and *endo* isomers, in ^{i}PrOH/H_2O, the amount of *endo* isomer was the highest found. This may be the factor explaining the highest conversion obtained in ^{i}PrOH/H_2O (Scheme 2).

The NMR spectra for the isomerization of 1,5-hexadien-3,4-diol are shown in Fig. S20–S31. Both catalysts tested were found to be inactive for its isomerization. In both solvents, D_2O and CD_3OD, the ^{31}P{^{1}H} NMR spectra of the reactions between 1,5-hexadien-3,4-diol and 10 mol% of **1** and **2** displayed the formation of eight doublets for **1** between −20.0 ppm and −25.0 ppm, and for **2** in the range of −6.0 to −9.0 ppm. The powder obtained by precipitation with Et_2O from these solutions displayed identical patterns in the ^{31}P{^{1}H} NMR spectra to

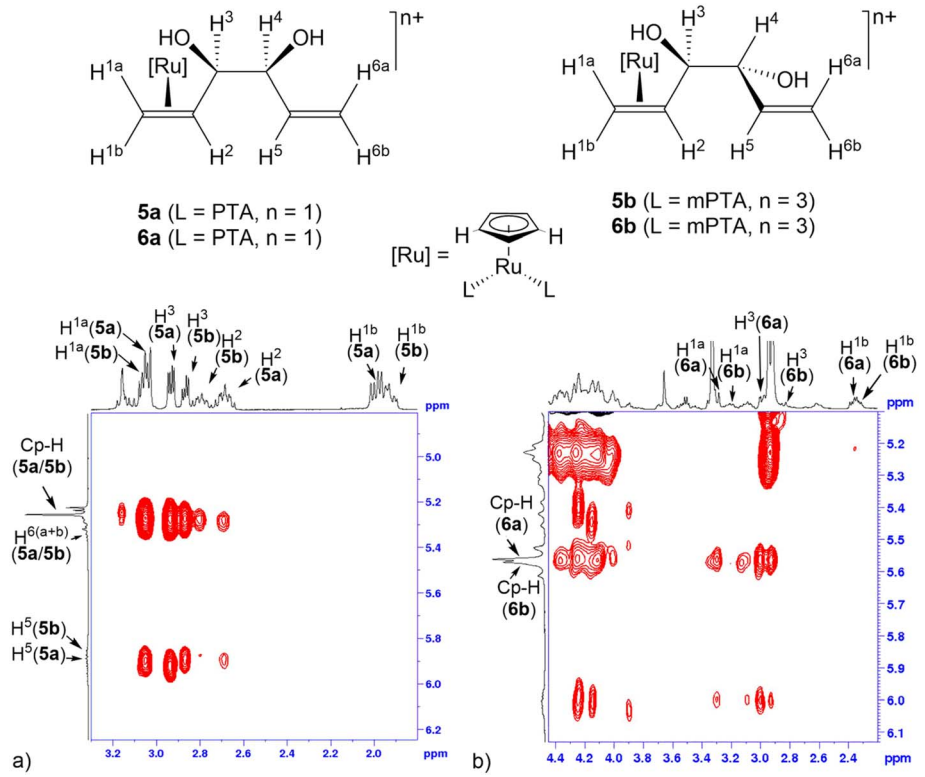

Fig. 2 Proposed structure for the isomers in solution **5a**, **5b**, **6a** and **6b**. (a) ROE cross peaks between Cp-H (**5a**/**5b**: 5.25 ppm) and H^{1a} (**5a**: 3.03 ppm; **5b**: 3.08 ppm) and H^3 (**5a**: 2.94 ppm; **5b**: 2.88 ppm); and ROE cross peaks between H^5 (**5a**: 5.89 ppm) and H^3 (**5a**: 2.94 ppm) and H^2 (**5a**: 2.68 ppm), and between H^5 (**5b**: 5.88 ppm) and H^{1a} (**5b**: 3.08 ppm) and H^3 (**5b**: 2.88 ppm). (b) ROE cross peaks between Cp-H (**6a**/**6b**: 5.56/5.57 ppm, respectively) and H^{1a} (**6a**: 3.29 ppm; **6b**: 3.22 ppm) and H^3 (**6a**: 2.99 ppm; **6b**: 2.96 ppm).

that obtained during the reactions, independently of the solvent D_2O and CD_3OD. Due to the strong signal overlap, it was only possible to characterize two of the major species given by each starting complex. The analysis of the ^1H–^1H COSY, ^1H–^{13}C HSQC, ^1H–^{13}C HMBC and finally ^1H–^1H ROESY spectra (**5**: Fig. S61–S70 and **6**: Fig. S71–S80) revealed that these species correspond to the complexes *exo*-[RuCp(η^2-(+/−)-CH_2═CH–CHOH–CHOH–CH═CH_2)(PTA)$_2$](CF_3SO_3) (**5a**), *exo*-[RuCp(η^2-*meso*-CH_2═CH–CHOH–CHOH–CH═CH_2)(PTA)$_2$](CF_3SO_3) (**5b**), *exo*-[RuCp(η^2-(+/−)-CH_2═CH–CHOH–CHOH–CH═CH_2)(mPTA)$_2$](CF_3SO_3)$_3$ (**6a**) and *exo*-[RuCp(η^2-*meso*-CH_2═CH–CHOH–CHOH–CH═CH_2)(mPTA)$_2$](CF_3SO_3)$_3$ (**6b**). The 1,5-hexadiane-3,4-diol disposition in all these species is an *exo*-η^2-C═C–Ru configuration, as confirmed by the ROESY ^1H–^1H NMR experiment (Fig. S70 and S80), given that the Cp-H protons belonging to complexes **5** and **6** are coupled to H^{1a}/H^3 (Fig. 2). The analysis of the $^3J_{H\text{-}H}$ coupling constants between the vicinal hydrogens H^3 and H^4 (**5a:** $^3J_{H\text{-}H}$ = 9.58 Hz; **5b:** $^3J_{H\text{-}H}$ = 12.20 Hz) suggests that the 1,5-hexadiane-3,4-diol ligand is syn in **5a** and anti in **5b**. Unfortunately, the signal overlapping prevented the measurement of the corresponding values for **6a** and **6b**. The overall results obtained for the reactions of **1** or **2** with 1,5-hexenadien-3,4-diol suggest that upon coordination to the catalyst, an *exo*-η^2-allylic complex is formed, which is stable enough to stop the isomerization reaction.

Fig. 3 illustrates the proposed mechanism for the studied catalytic isomerization reactions. In addition, the highest turnover numbers for each aqueous isomerization reaction catalysed by both complexes are depicted, highlighting substrate-dependent differences. Overall, the lower catalytic activity of **2** compared to **1** is consistent with previous published results.[20,22,23,72] All the pieces of information collected across this study suggest some important facts, as follows: (a) the composition of the solvent mixture plays a crucial role in the process

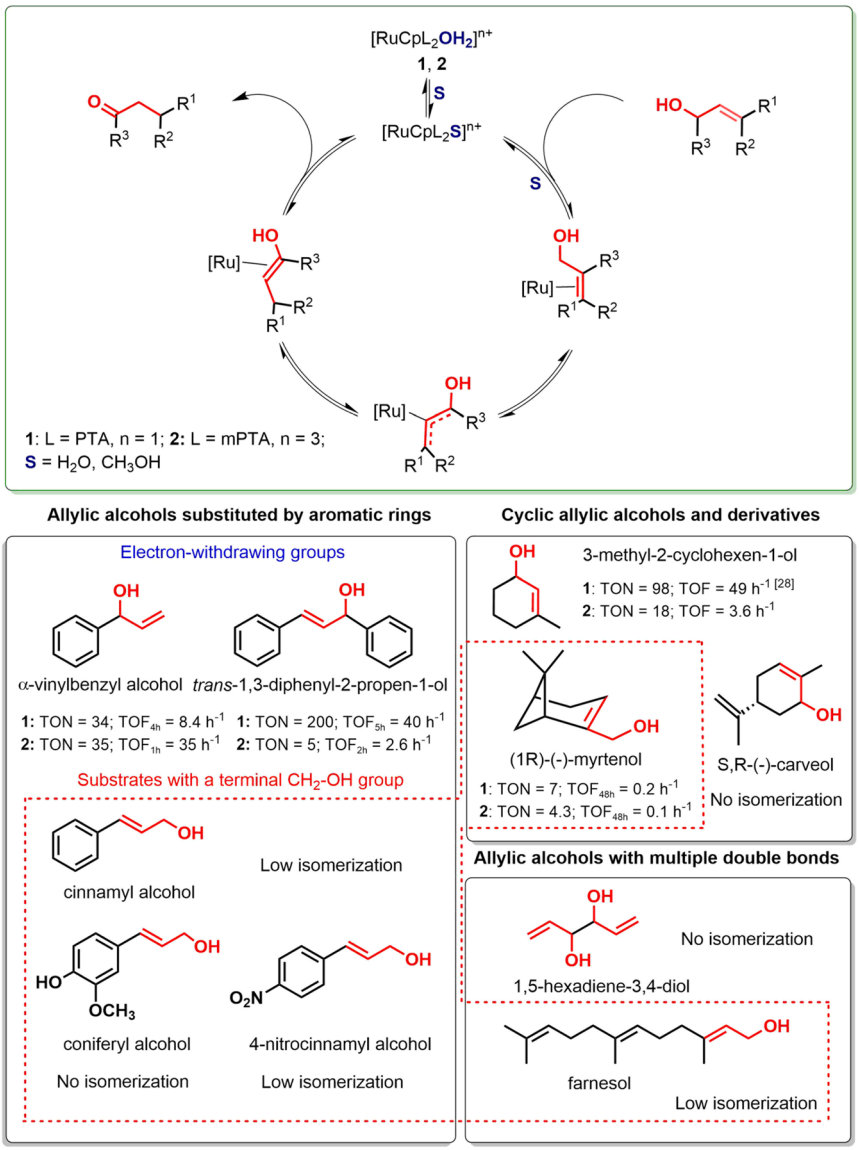

Fig. 3 Proposed mechanism for the aqueous isomerization of the studied allylic alcohols catalyzed by the water-soluble complexes **1** and **2**.

and (b) an electron-withdrawing group in the allylic position appears to aid the isomerisation process. Particularly, the presence of water facilitates the conversion of the active *exo*-isomer in the isomerization process into the inactive *endo*-isomer, which was also found for the catalytic activity of **1** and **2** with linear and cyclic allylic alcohols.[24] Conversely, the stabilization of the substrate in an inactive conformation (**5a**, **5b**, **6a** and **6b**) could be also the reason for the null conversion of 1,5-hexadiane-3,4-diol. Also, the results showed that bulky-substituted substrates with an electron-withdrawing group in the vinylic position and with a terminal CH_2–OH group are poorly isomerised.[72]

Conclusions

The catalytic activity of the $[RuCp(OH_2)(PTA)_2](CF_3SO_3)$ (**1**) and $[RuCp(OH_2)(mPTA)_2](CF_3SO_3)_3$ (**2**) complexes was assessed for the isomerization of the substituted allylic alcohols *trans*-1,3-diphenyl-2-propen-1-ol, vinylbenzyl alcohol, 3-methyl-2-cyclohexen-1-ol, (1*R*)-(−)-myrtenol, cinnamyl alcohol, 4-nitrocinnamyl alcohol, farnesol, coniferyl alcohol, *S*,*R*-(−)-carveol and 1,5-hexadien-3,4-diol in water and aqueous media. The catalytic activity of **1** was notable for the isomerization of *trans*-1,3-diphenyl-2-propen-1-ol into dihydrochalcone (TON = 200, TOF_{5h} = 40 h^{-1}), α-vinylbenzyl alcohol into propiophenone (TON = 34, TOF_{4h} = 8.4 h^{-1}), and 3-methyl-2-cyclohexen-1-ol into 3-methylcyclohexanone (TON = 285, TOF_{15h} = 19), while only modest activity was observed for the isomerization of (1*R*)-(−)-myrtenol into myrtanal (TON = 7, TOF_{48h} = 0.2 h^{-1}). In contrast, complex **2** exhibited good efficiency for the synthesis of propiophenone (TON = 35, TOF_{1h} = 35 h^{-1}) and moderate activity for the synthesis of 3-methylcyclohexanone (TON = 18, TOF_{5h} = 3.6). The remaining substrates were not isomerized.

Notably, the products obtained are key natural products, which have distinct roles across the pharmaceutical, synthetic, cosmetic, and food industries and pest management. Dihydrochalcone offers antimicrobial and anti-inflammatory properties and is also used in the food industry as a sweetener.[46,51,73,74] To the best of our knowledge, the obtained isomerization conversion of *trans*-1,3-diphenyl-2-propen-1-ol catalyzed by **1** (TON = 200 and TOF_{5h} = 40 h^{-1}) into dihydrochalcone is the highest known in aqueous medium to date. Propiophenone is a key intermediate for synthesizing drugs such as antidepressants and stimulants.[44,45,75–78] Furthermore, it is an essential intermediate in complex drug synthesis and valued in cosmetics for its fragrances. Myrtanal possesses antioxidant and antiseptic properties,[79,80] and 3-methylcyclohexanone has a potential role as an anti-aggregation agent, which along with 1-methyl-2-cyclohexen-1-ol and 3-methyl-2-cyclohexenone, the 1,3-transposition and oxidation products of 3-methyl-2-cyclohexen-1-ol, respectively, are pheromones used in the natural aggregation/anti-aggregation system of the Douglas-fir beetle.[39]

The obtained results support the hypothesis that the size and substitution of allylic alcohols influence the isomerization conversion, revealing that these complexes are more effective for isomerising branched substrates with electron-withdrawing groups in the allylic position, such as in *trans*-1,3-diphenyl-2-propen-1-ol and α-vinylbenzyl alcohol. Additionally, substrates with a CH_2OH terminal group such as cinnamyl alcohol, coniferyl alcohol and 4-nitrocinnamyl alcohol, were poorly converted. Steric hindrance, particularly from bulky groups and the methyl group in the vinyl position, may hinder the coordination to ruthenium. The combination of both steric hindrance and the presence of a CH_2OH terminal group seemed to impede the isomerization of (1*R*)-(−)-myrtenol. Additionally, mechanistic studies confirmed the formation of the $[RuCp(\eta^2\text{-}CH_2{=}CH{-}CHOH{-}C_6H_5)(PTA)_2](CF_3SO_3)$ (**3**) and $[RuCp(\eta^2\text{-}CH_2{=}CH{-}CHOH{-}C_6H_5)(mPTA)_2](CF_3SO_3)_3$ (**4**) intermediates during the isomerization of α-vinylbenzyl alcohol. These findings support the proposed thermodynamic equilibrium of the η^2-allylic-alcohol-intermediates (*exo* → *endo)* preceding the isomerization. Additionally, the low reactivity of 1,5-hexadien-3,4-diol was attributed to the formation of inactive intermediates, which probably block the reaction.

Conflicts of interest

The authors declare no conflict of interest.

Data availability

Supporting data have been included in the article's SI. See DOI: **https://doi.org/10.1039/d5ra03564c**.

Acknowledgements

The authors thank Junta de Andalucía for funding the group PAI FQM-317 and the University of Almería for the project P_LANZ_2023/006 and P_FORT_GRUPOS_2023/94 (both projects co-funded by the European Commission FEDER program).

References

1 F. Scalambra, P. Lorenzo-Luis, I. de los Rios and A. Romerosa, *Coord. Chem. Rev.*, 2019, **393**, 118–148.
2 D. Cahard, S. Gaillard and J. L. Renaud, *Tetrahedron Lett.*, 2015, **56**, 6159–6169.
3 J. García-Álvarez, J. Gimeno and F. J. Suárez, *Organometallics*, 2011, **30**, 2893–2896.
4 R. Uma, C. Crévisy and R. Grée, *Chem. Rev.*, 2002, **103**, 27–51.
5 L. Mantilli, D. Gérard, S. Torche, C. Besnard and C. Mazet, *Angew. Chem., Int. Ed.*, 2009, **48**, 5143–5147.
6 X. X. Zhang, Y. Zhang, L. Liao, Y. Gao, H. E. M. Su and J. S. Yu, *ChemCatChem*, 2022, **14**, e202200126.
7 N. Ahlsten, H. Lundberg and B. Martín-Matute, *Green Chem.*, 2010, **12**, 1628–1633.
8 T. Campos-Malpartida, M. Fekete, F. Joó, Á. Kathó, A. Romerosa, M. Saoud and W. Wojtków, *J. Organomet. Chem.*, 2008, **693**, 468–474.
9 E. Bolyog-Nagy, A. Udvardy, Á. Barczáné-Bertók, F. Joó and Á. Kathó, *Inorg. Chim. Acta*, 2017, **455**, 514–520.

10 A. Mena-Cruz, M. Serrano-Ruiz, P. Lorenzo-Luis, A. Romerosa, Á. Kathó, F. Joó and L. M. Aguilera-Sáez, *J. Mol. Catal. A:Chem.*, 2016, **411**, 27–33.
11 A. B. Gómez, P. Holmberg, J. E. Bäckvall and B. Martín-Matute, *RSC Adv.*, 2014, **4**, 39519–39522.
12 A. E. Díaz-Álvarez, P. Crochet, M. Zablocka, C. Duhayon, V. Cadierno, J. Gimeno and J. P. Majoral, *Adv. Synth. Catal.*, 2006, **348**, 1671–1679.
13 F. Joó, J. Kovács, Á. Kathó, A. C. Bényei, T. Decuir, D. J. Darensbourg, A. Miedaner and D. L. Dubois, (Meta-Sulfonatophenyl) Diphenylphosphine, Sodium Salt and its Complexes with Rhodium(I), Ruthenium(II), Iridium(I), in *Inorganic Synthesis*, John Wiley & Sons, Ltd, 2007, vol. 32, pp. 1–8.
14 A. D. Phillips, L. Gonsalvi, A. Romerosa, F. Vizza and M. Peruzzini, *Coord. Chem. Rev.*, 2004, **248**, 955–993.
15 J. Bravo, S. Bolaño, L. Gonsalvi and M. Peruzzini, *Coord. Chem. Rev.*, 2010, **254**, 555–607.
16 A. Guerriero, M. Peruzzini and L. Gonsalvi, *Coord. Chem. Rev.*, 2018, **355**, 328–361.
17 D. N. Akbayeva, L. Gonsalvi, W. Oberhauser, M. Peruzzini, F. Vizza, P. Brüggeller, A. Romerosa, G. Sava and A. Bergamo, *Chem. Commun.*, 2003, **2**, 264–265.
18 M. Serrano-Ruiz, L. M. Aguilera-Sáez, P. Lorenzo-Luis, J. M. Padrón and A. Romerosa, *Dalton Trans.*, 2013, **42**, 11212–11219.
19 A. Romerosa, T. Campos-Malpartida, C. Lidrissi, M. Saoud, M. Serrano-Ruiz, M. Peruzzini, J. A. Garrido-Cárdenas and F. García-Maroto, *Inorg. Chem.*, 2006, **45**, 1289–1298.
20 B. González, P. Lorenzo-Luis, P. Gili, A. Romerosa and M. Serrano-Ruiz, *J. Organomet. Chem.*, 2009, **694**, 2029–2036.
21 B. González, P. Lorenzo-Luis, M. Serrano-Ruiz, É. Papp, M. Fekete, K. Csépke, K. Ősz, Á. Kathó, F. Joó and A. Romerosa, *J. Mol. Catal. A:Chem.*, 2010, **326**, 15–20.
22 M. Serrano-Ruiz, P. Lorenzo-Luis, A. Romerosa and A. Mena-Cruz, *Dalton Trans.*, 2013, **42**, 7622.
23 F. Scalambra, M. Serrano-Ruiz and A. Romerosa, *Dalton Trans.*, 2017, **46**, 5864–5871.
24 F. Scalambra, B. Lopez-Sanchez, N. Holzmann, L. Bernasconi and A. Romerosa, *Organometallics*, 2020, **39**, 4491–4499.
25 F. Scalambra, B. López-Sanchez and A. Romerosa, *Dalton Trans.*, 2018, **47**, 16398–16402.
26 B. López-Sánchez, F. Scalambra and A. Romerosa, *Appl. Organomet. Chem.*, 2024, e7368.
27 B. López-Sánchez, A. B. Bohome-Espinosa, F. Scalambra and A. Romerosa, *Appl. Organomet. Chem.*, 2022, **37**, e6971.
28 D. L. Six and R. Bracewell, *Bark Beetles: Biology and Ecology of Native and Invasive Species*, 2015, pp. 305–350.
29 G. Chen, Y. Song, P. Wang, J. Chen, Z. Zhang, S. Wang, X. Huang and Q. H. Zhang, *Chemoecology*, 2015, **25**, 135–145.
30 R. L. Isitt, K. P. Bleiker, D. S. Pureswaran, N. K. Hillier and D. P. W. Huber, *J. Chem. Ecol.*, 2020, **46**, 497–507.
31 R. L. Isitt, K. P. Bleiker, D. S. Pureswaran, N. K. Hillier and D. P. W. Huber, *Environ. Entomol.*, 2018, **47**, 1293–1299.
32 B. D. Johnston, B. Morgan, A. C. Oehlschlager and S. Ramaswamy, *Tetrahedron:Asymmetry*, 1991, **2**, 377–380.
33 D. W. Ross and G. E. Datermanl, *J. Econ. Entomol.*, 1995, **88**, 106–111.
34 D. P. W. Huber and J. H. Borden, *J. Chem. Ecol.*, 2001, **27**, 217–233.
35 K. Mori, B. G. Hazra, R. J. Pfeiffer, A. K. Gupta and B. S. Lindgren, *Tetrahedron*, 1987, **43**, 2249–2254.
36 L. C. Ryker, L. M. Libbey and J. A. Rudinsky, *Environ. Entomol.*, 1979, **8**, 789–798.
37 D. S. Pureswaran and J. H. Borden, *Chemoecology*, 2004, **14**, 67–75.
38 J. A. Rudınsky, L. N. Kline and J. D. Diekman, *J. Econ. Entomol.*, 1975, **68**, 527–528.
39 N. Bakthavatsalam, *Ecofriendly Pest Management for Food Security*, 2016, pp. 563–611.
40 R. A. Savidge and H. Förster, *Phytochemistry*, 2001, **57**, 1095–1103.
41 D. Tatman and H. Mo, *Cancer Lett.*, 2002, **175**, 129–139.
42 B. Schilling, R. Kaiser, A. Natsch and M. Gautschi, *Chemoecology*, 2010, **20**, 135–147.
43 T. Hennebelle, S. Sahpaz, C. Dermont, H. Joseph and F. Bailleul, *Chem. Biodiversity*, 2006, **3**, 1116–1125.
44 A. S. Awaad, N. A. Al-Jaber, G. A. Soliman, M. R. Al-Outhman, M. E. Zain, J. E. Moses and R. M. El-Meligy, *Phytother. Res.*, 2012, **26**, 452–457.
45 R. Costa, M. R. De Fina, M. R. Valentino, A. Rustaiyan, P. Dugo, G. Dugo and L. Mondello, *Flavour Fragrance J.*, 2009, **24**, 75–82.
46 F. A. Tomás-Barberán and M. N. Clifford, *J. Sci. Food Agric.*, 2000, **80**, 1073–1080.
47 R. Ramachanderan and B. Schaefer, *ChemTexts*, 2019, **5**, 1–34.
48 C. S. Letizia, J. Cocchiara, J. Lalko, A. Lapczynski and A. M. Api, *Food Chem. Toxicol.*, 2005, **43**, 837–866.
49 A. Engelhardt, D. Jerchel, H. Weidmann and H. Wick, *Naunyn Schmiedebergs Arch Exp Pathol Pharmakol*, 1958, vol. 235, pp. 10–18.
50 M. Gálvez-Llompart, R. Zanni, P. Romualdi and R. García-Domenech, *Med. Chem. Res.*, 2013, **22**, 3466–3477.
51 X. M. Chen, W. Q. Yang, X. Wang, C. Chen, Z. M. Qian, S. M. Wang and D. Tang, *Food Funct.*, 2022, **13**, 5899–5913.
52 M. Tomoeda, *Pharm. Bull.*, 1957, **5**, 335–342.
53 B. Schmidt and L. Staude, *J. Org. Chem.*, 2011, **76**, 2220–2226.
54 A. M. Api, D. Belsito, D. Botelho, M. Bruze, G. A. Burton, J. Buschmann, M. L. Dagli, M. Date, W. Dekant, C. Deodhar, M. Francis, A. D. Fryer, L. Jones, K. Joshi, S. La Cava, A. Lapczynski, D. C. Liebler, D. O'Brien, A. Patel, T. M. Penning, G. Ritacco, J. Romine, N. Sadekar, D. Salvito, T. W. Schultz, I. G. Sipes, G. Sullivan, Y. Thakkar, Y. Tokura and S. Tsang, *Food Chem. Toxicol.*, 2019, **130**, 110602.
55 S. P. Bhatia, D. McGinty, C. S. Letizia and A. M. Api, *Food Chem. Toxicol.*, 2008, **46**, S237–S240.
56 M. R. C. Moreira, M. G. S. S. Salvadori, A. A. C. de Almeida, D. P. de Sousa, J. Jordán, P. Satyal, R. M. de Freitas and R. N. de Almeida, *Neurosci. Lett.*, 2014, **579**, 119–124.

57 M. R. V. Santos, F. V. Moreira, B. P. Fraga, D. P. de Sousa, L. R. Bonjardim and L. J. Quintans, *Rev. Bras. Farmacogn.*, 2011, **21**, 764–771.
58 R. O. Silva, M. S. Salvadori, F. B. M. Sousa, M. S. Santos, N. S. Carvalho, D. P. Sousa, B. S. Gomes, F. A. Oliveira, A. L. R. Barbosa, R. M. Freitas, R. N. de Almeida and J. V. R. Medeiros, *Flavour Fragrance J.*, 2014, **29**, 184–192.
59 A. W. Archer, *J. Chromatogr. A*, 1988, **447**, 272–276.
60 Z. Rao, F. Xu, T. Wen, F. Wang, W. Sang and N. Zeng, *Biomed. Pharmacother.*, 2018, **101**, 304–310.
61 X. Lan and T. Wang, *ACS Catal.*, 2020, **10**, 2764–2790.
62 V. Cadierno, S. E. García-Garrido, J. Gimeno, A. Varela-Álvarez and J. A. Sordo, *J. Am. Chem. Soc.*, 2006, **128**, 1360–1370.
63 J. Schulz, I. Císařová and P. S. Těpnička, *Eur. J. Inorg. Chem.*, 2012, 5000–5010.
64 L. Bellarosa, J. Díez, J. Gimeno, A. Lledós, F. J. Suárez, G. Ujaque and C. Vicent, *Chem.–Eur. J.*, 2012, **18**, 7749–7765.
65 J. Díez, J. Gimeno, A. Lledós, F. J. Suárez and C. Vicent, *ACS Catal.*, 2012, **2**, 2087–2099.
66 N. Ríos-Lombardía, C. Vidal, E. Liardo, F. Morís, J. García-Álvarez and J. González-Sabín, *Angew. Chem., Int. Ed.*, 2016, **55**, 8691–8695.
67 N. Ríos-Lombardía, C. Vidal, M. Cocina, F. Morís, J. García-Álvarez and J. González-Sabín, *Chem. Commun.*, 2015, **51**, 10937–10940.
68 V. Cadierno, S. E. García-Garrido and J. Gimeno, *Chem. Commun.*, 2004, **4**, 232–233.
69 H. M. R. Hoffmann, A. Köver and D. Pauluth, *J. Chem. Soc. Chem. Commun.*, 1985, 812–814.
70 B. J. Frost and C. A. Mebi, *Organometallics*, 2004, **23**, 5317–5323.
71 C. A. Mebi, R. P. Nair and B. J. Frost, *Organometallics*, 2007, **26**, 429–438.
72 F. Scalambra, N. Holzmann, L. Bernasconi, S. Imberti and A. Romerosa, *ACS Catal.*, 2018, **8**, 3812–3819.
73 M. Jung, S. Triebel, T. Anke, E. Richling and G. Erkel, *Mol. Nutr. Food Res.*, 2009, **53**, 1263–1280.
74 C. Rivière, in *Studies in Natural Products Chemistry*, Elsevier, 2016, vol. 51, pp. 253–381.
75 J. Q. Wang, Z. S. Dai, Y. Gao, F. Wang, J. X. Chen, Z. H. Feng, J. F. Yin, L. Zeng and Y. Q. Xu, *LWT*, 2023, **185**, 115128.
76 S. Dagdelen, T. Bilenler, G. Durmaz, I. Gokbulut, A. A. Hayaloglu and I. Karabulut, *J. Food Process. Preserv.*, 2014, **38**, 1716–1725.
77 Ü. Demir Özkay, L. Yurttaş, Y. Özkay, U. I. Üçel, Ö. D. Can and Y. Öztürk, *Arch. Pharmacal Res.*, 2013, **36**, 802–811.
78 *Novel Process For The Preparation of R-Phenylacetylcarbinol and β-Aminoalcohols*, WO2020129087A1, **https://patents.google.com/patent/WO2020129087A1/en**, accessed 5 March 2025.
79 V. Papandreou, P. Magiatis, I. Chinou, E. Kalpoutzakis, A. L. Skaltsounis and A. Tsarbopoulos, *J. Ethnopharmacol.*, 2002, **81**, 101–104.
80 V. Klontza, K. Graikou, A. Cheilari, V. Kasapis, C. Ganos, N. Aligiannis and I. Chinou, *Int. J. Mol. Sci.*, 2023, **24**, 4935.